

Supporting Information

Zn_{0.5}Cd_{0.5}Se quantum dots integrated MOF derived C/N-CeO₂ photocatalyst for enhanced H₂O₂ production and O₂ evolution reactions

Jayashree Panda^a, Jyotirmayee Sahu^a, Kulamani Parida^{a*}

^aCentre for Nano Science and Nanotechnology, Siksha “O” Anusandhan (Deemed to be University), Bhubaneswar-751030, Odisha, India

E-mail: Corresponding author: kulamaniparida@soa.ac.in

Supporting Information Contents:

No. of Pages: 19

No. of Figures: 12

No. of Tables: 07

No of equation: 03

1. Materials and methods:

1.1 Chemicals utilized: Cerium chloride ($\text{CeCl}_3 \cdot 7\text{H}_2\text{O}$), 2-Amino-1, 4-benzene dicarboxylic acid [$\text{H}_2\text{BDC-NH}_2$], Zinc acetate ($\text{Zn}(\text{OAc})_2 \cdot 2\text{H}_2\text{O}$), Cadmium acetate ($\text{Cd}(\text{OAc})_2 \cdot 2\text{H}_2\text{O}$), Se powder, TA (Terephthalic Acid), NBT (nitro blue tetrazolium chloride), Nafion, citric acid (CA), dimethyl sulphoxide (DMSO), Na_2SO_4 , tert-Butyl alcohol (TBA), Isopropyl alcohol (IPA), and Thioglycolic acid (TGA) were purchased from sigma Aldrich. Methanol, Ethanol, Isopropanol, p-benzoquinone (p-BQ) and N, N- Dimethyl formamide (DMF) were obtained from MERCK and are used without further purification.

1.2 Synthesis Route of C/N-CeO₂, ZCSe, and C/N-CeO₂@ZCSe:

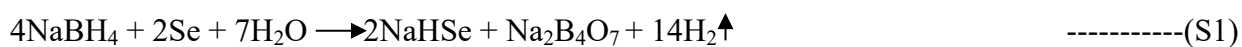
1.2.1 Synthesis Route of Ce-MOF and derived C/N-CeO₂:

Ce based secondary building units (SBUs) coordinated with amine ($-\text{NH}_2$) group functionalized BDC linkers to prepare the MOF which is synthesised by hydrothermal technique. In this preparation strategy, 0.74 g of $\text{CeCl}_3 \cdot 7\text{H}_2\text{O}$ and 0.36 g of $\text{H}_2\text{BDC-NH}_2$ were dissolved in 30 mL of DMF separately, followed by each solution being stirred (30 min) to obtain Ce-metal and BDC-NH₂ ligand precursor solution for MOF preparation. The obtained Ce salt solution was mixed with the prepared $\text{H}_2\text{BDC-NH}_2$ solution and subjected to stirring for 60 min. Then, the pale-yellow suspension was transferred into a Teflon-lined stainless-steel autoclave and kept in the hot air oven for 24 h at 150 °C for hydrothermal treatment. Subsequently the autoclave was allowed to cool down naturally, and the sample was collected by centrifugation. Further, the obtained product was activated in methanol and washed several times with methanol (to remove unreacted metal salts and ligands). Thereafter, the material was dried overnight at 343 K and finally the off white-coloured sample was ground and labelled as Ce-MOF. To synthesize the C/N-CeO₂ photocatalysts, the as-prepared Ce-MOFs were calcined in a muffle furnace for 2 h at a heating rate of 5 °C min⁻¹ from room temperature (RT, 25°C) to 450 °C under ambient air atmosphere.

1.2.2. Synthesis Route of ZnCdSe alloyed quantum dots:

$\text{Zn}_{0.5}\text{Cd}_{0.5}\text{Se}$ (ZCSe-1) alloyed QDs were fabricated by a one pot method by following previously reported literature with slight modification. Briefly, NaHSe solutions as Se precursor were synthesized by dissolving Se powder with NaBH_4 in chilled water. 0.12g (3 mmol) of NaBH_4 was dissolved in 2 mL of chilled distilled water in a flask, followed by the addition of 0.079g (1

mmol) of Se powder. Immediately the flask was placed into an ice bath and H₂ gas was bubbled for approximately 60 to 90 min. Finally, the black Se was reduced to transparent NaHSe, and white Na₂B₄O₇ precipitated.



For the typical synthesis of ZCSe-1 QDs with 0.5 : 0.5 molar ratio of Zn : Cd, Zn(OAc)₂·2H₂O (0.115g), Cd(OAc)₂·2H₂O (0.135 g) and TGA (0.5 mL) were dissolved in 100 mL deionized water in a three-neck round bottomed flask with continuous stirring. The pH was adjusted around 11 by 0.1 M NaOH under an N₂ atmosphere to prevent oxidation of the material. The freshly synthesized NaHSe was quickly added into the solution and kept refluxing at 100 °C for 3 h. Finally, the resultant products were settled down keeping undisturbed for overnight and was then centrifuged and washed with water and ethanol each three times, followed by drying in an oven to form ZCSe QDs.

1.2.3. Synthesis Route of C/N-CeO₂/ZCSe (CZCSe-x) Heterostructure:

For the synthesis of composites CZCSe-x, first of all, 0.2 g of the as-synthesised C/N-CeO₂ was dispersed in 50 mL of distilled water through ultrasonication for almost 30 minutes. Meanwhile, in another beaker NaHSe solutions as Se precursor were synthesized by dissolving Se powder with NaBH₄ in chilled water. 0.12g (3 mmol) of NaBH₄ was dissolved in 2 mL of chilled distilled water in a flask, followed by the addition of 0.079g (1 mmol) of Se powder. Immediately the flask was placed into an ice bath and H₂ gas was bubbled for approximately 60 to 90 min. Then, For the typical synthesis of ZCSe-1 QDs with 0.5 : 0.5 molar ratio of Zn : Cd, Zn(OAc)₂·2H₂O (0.115g), Cd(OAc)₂·2H₂O (0.135 g) and TGA (0.5 mL) were dissolved in 100 mL deionized water in a three-neck round bottomed flask (3RB) with continuous stirring. The pH was adjusted around 11 by 0.1 M NaOH under an N₂ atmosphere to prevent oxidation of the material. The freshly synthesized NaHSe was quickly added into the solution. Thereupon, the aqueous solution of C/N-CeO₂ was added slowly in to the 3RB and kept refluxing at 100 °C for 3 h. Finally, the resultant products were settled down keeping undisturbed for overnight and was then centrifuged and washed with water and ethanol each three times, followed by drying in an oven to form the 0.5, 1, and 1.5 mmol ZCSe decorated on C/N-CeO₂, C/N-CeO₂/ZCSe composites denoted as CZCSe-x where, x = 0.5, 1, 1.5 respectively. The schematic synthesis protocol of all fabricated photocatalysts was displayed in scheme-1.

2. Characterization Details:

2.1. Physicochemical Characterization:

X-ray diffraction study (XRD) of prepared samples were estimated in 2θ range of 5° - 80° by Rigaku Ultima IV instrument equipped with Cu $K\alpha$ X-ray source ($\lambda = 0.154$ nm). JASCO V-750 spectrophotometer was used to study the optical property of synthesized samples, taking $BaSO_4$ as the reference. Morphology and internal topological behavior of C/N- CeO_2 , ZCSe, and C/N- CeO_2 /ZCSe was determined via ZEISS SUPRA-55 (Scanning electron microscopy (SEM) and JEOL JEM 2100 (Transmission electron microscopy (TEM) instruments. VG microtech multilab ESCA 3000 spectrometers fitted with Mg- $K\alpha$ -X-ray source for XPS characterization and ICP-OES analysis was performed with the help of Elementar Vario EL III Carlo Erba 1108 elemental analyser to investigate the binding energy change and determine the wt % of element present in target photo catalyst respectively. Surface texture i.e. N_2 adsorption desorption, surface area and pore distribution of prepared photocatalyst was analysed by NOVA2200e, Quantachrome Apparatus at de-gassing temperature $200^{\circ}C$ for 7 hrs. Agilent 7890B GC and the column is HP-5MS was used for GC-analysis of target product i.e. biphenyl. Multi-channel IVIUMnSTAT was used for electrochemical characterization of the synthesized photo catalyst in presence of 0.1 M Na_2SO_4 aqueous solution. Light radiance can be performed by using 300 W Xenon lamps equipped with a 400 nm cut-off filter.

2.2 Electrochemical characterization:

Working electrodes were prepared using the drop casting process over fluorine doped tin oxide (FTO) glass. The FTOs were first thoroughly cleaned using ultrasonication in deionized water and ethanol before being dried in a hot air oven at $100^{\circ}C$. The sample was then applied to the conducting surface of the FTO (1 mg photocatalyst, 1.4 mL ethanol, 40 μ L nafion, and 1.6 mL distilled water, all sonicated for 30 min). A typical three-electrode cell is used for electrochemical measurements, with the platinum electrode serving as a counter, the saturated Ag/AgCl electrode serving as the reference electrode, and the sample coated FTO serving as the working electrodes, respectively. The entire analysis was completed in an aqueous solution of 0.1 M Na_2SO_4 .

3. Photocatalytic Experimental Setup:

The above synthesized materials were carried out for two types of photocatalytic applications as explained below:

3.1. Photocatalytic H₂O₂ production setup:

The photocatalytic H₂O₂ production reaction of C/N-CeO₂, ZCSe, and CZCSe-x photocatalysts was carried out in an oxygen saturated atmosphere under light irradiation for 2 hour. For this H₂O₂ evolution experiment, 20 mg of each photocatalyst were dispersed in 20 mL of solution (18 mL DI + 2 mL Isopropanol) followed by ultrasonication for 15 minutes. Furthermore, at room temperature only, the solution was illuminated with 250 W Hg-lamp followed by oxygen purging for 45 minutes. The suspension was centrifuged and filtered to obtain clear filtrate for analysis after 2 h of photocatalytic reaction. After that, 2 mL of clear filtrate was mixed with 2 mL of 0.1 M potassium iodide and 0.05 mL of 0.01 M ammonium molybdate solution for colour generation before running the spectra. Keeping at rest in dark for 5-10 minutes, the resultant mixture was analysed using a UV-Vis spectrophotometer centred at 350 nm.

3.2. Photocatalytic Water Oxidation Reaction setup:

Further the photocatalytic water oxidation activity was evaluated for the as synthesised material using another reactor fitted with a chiller and a light source. For this experiment, 20 mg of catalyst was poured in the quartz container and 20 mL of 0.05 M AgNO₃ solution was added to it, followed by stirring for 30 minutes in dark condition in order to maintain the adsorption-desorption equilibrium. After that, N₂ gas was bubbled through the solution for 30 minutes for deaeration purpose to ensure the oxygen evolved during the processes is due to water splitting reaction only. Further, a 150 W Xe arc lamp was used as light source to irradiate light in the suspension for 1 h. Then, the produced oxygen was quantified by an Agilent 7890b-series GC instrument equipped with the necessary items. Moreover, the apparent conversion efficiency (ACE) for O₂ evolution and solar to chemical conversion efficiency (SCC) for H₂O₂ production using the best photocatalyst was evaluated with detailed calculation as below.

4. (a) Calculation of Apparent Conversion Efficiency (ACE)

ACE of CZCSe-1 composite towards O₂ evolution (234.89 mmol h⁻¹) under light irradiation (150W Xe arc lamp) was calculated by the formula as stated below. [S2]

$$\text{ACE} = \frac{\text{Stored chemical energy (SCE)}}{\text{Incident light Intensity (ILI)}} \quad \text{-----}$$

(S2)

$$\begin{aligned} \text{SCE} &= \text{No. of moles of O}_2 \text{ produced per sec} * \text{Heat of combustion in kJ/mole } (\Delta H_c \text{ of O}_2) \\ &= 0.06525 * 10^{-6} \text{ mole/sec} * 285.8 * 10^3 \text{ J/mole} \\ &= 18.648 * 10^{-3} \text{ J/sec} \end{aligned}$$

$$= 0.01864 \text{ W}$$

ILI = Intensity of used Hg lamp * Distance of lamp from solution * Surface area of the spherical region (πr^2) on which light is focused

$$= 70 \text{ mW/cm}^2 * 3.14 * (1.5 \text{ cm})^2$$

$$= 494.55 \text{ mW}$$

$$= 0.4945 \text{ W}$$

$$\text{ACE} = \frac{0.01864 \text{ W}}{0.4945 \text{ W}} = 3.76 \%$$

(b) Calculation of solar to chemical conversion efficiency (SCC %)

SCC of CZCSe-1 towards H_2O_2 generation under 250 W Hg-lamp can be calculated by following the equation below [S3]:

$$\text{SCC \%} = \frac{\Delta G^\circ \text{ for } \text{H}_2\text{O}_2 \text{ generation} \left(\frac{\text{J}}{\text{mol}} \right) \times \text{H}_2\text{O}_2 \text{ produced (mol)}}{\text{Input energy (W)} \times \text{reaction time (s)}} \times 100$$

-----(S3)

Further, for H_2O_2 evolution, ΔG° is $117 \text{ kJ} \cdot \text{mol}^{-1}$. The irradiance of 250 W Hg-lamp is 1.33 W cm^{-2} and irradiated area is 127.2 cm^2 . In a 1 h of reaction time, the amount of H_2O_2 produced is $56.40 \mu\text{mol}$.

$$\text{Input Energy (W)} = \text{Irradiance (W cm}^{-2}\text{)} * \text{Irradiated area (cm}^2\text{)}$$

$$= 1.33 * 127.2$$

$$= 169.14 \text{ W}$$

Putting all these in equation [S3], the SCC efficiency is calculated to be 0.11%.

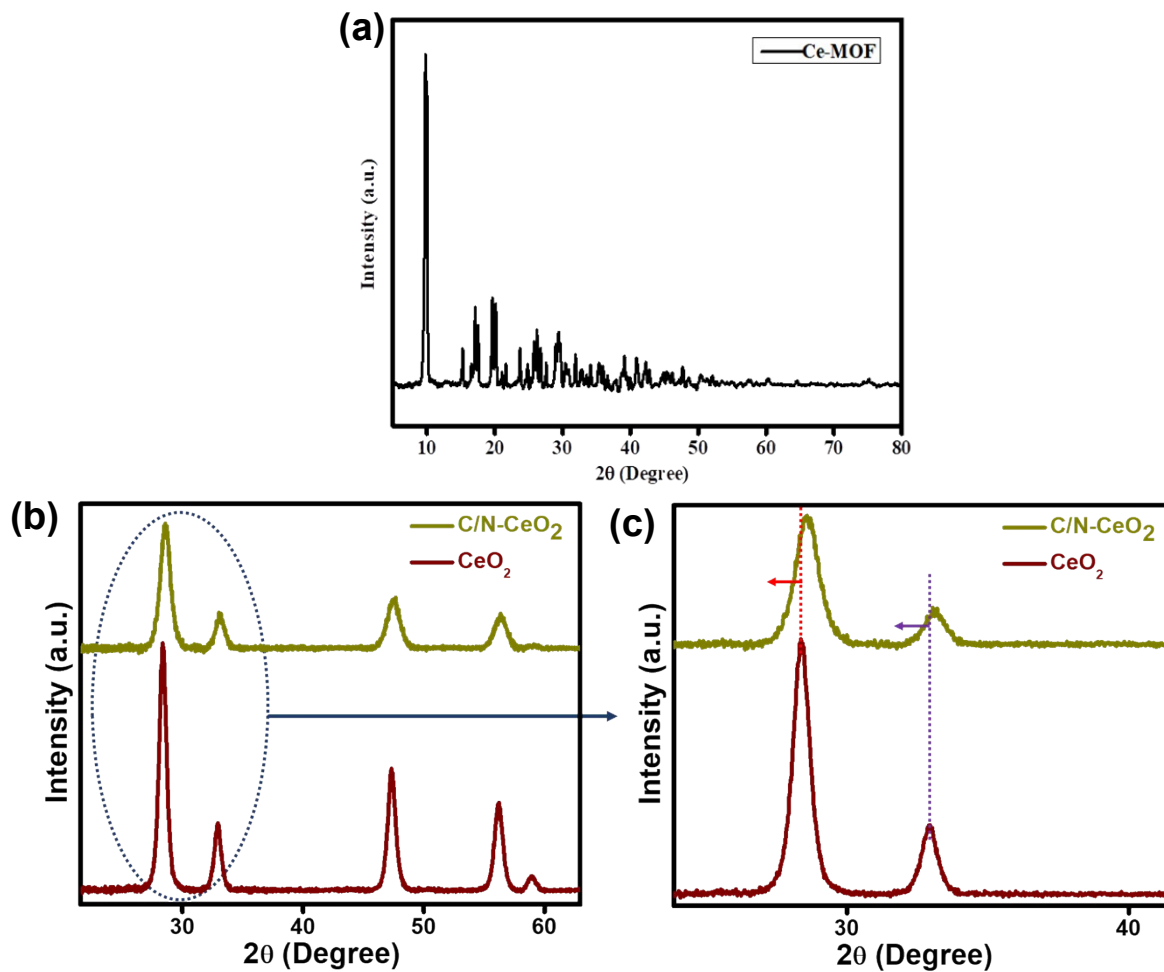


Fig. S1. (a) XRD spectrum of Ce-MOF, (b, c) comparison XRD and zoomed XRD spectra of C/N-CeO₂ and CeO₂

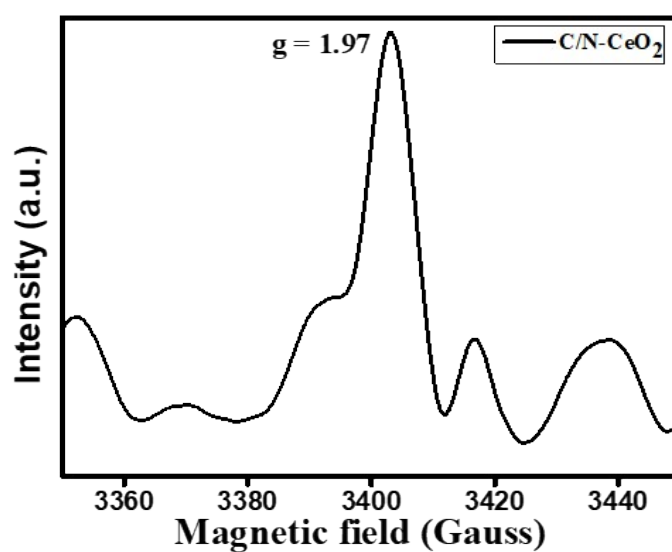


Fig. S2. EPR Spectrum of C/N-CeO₂

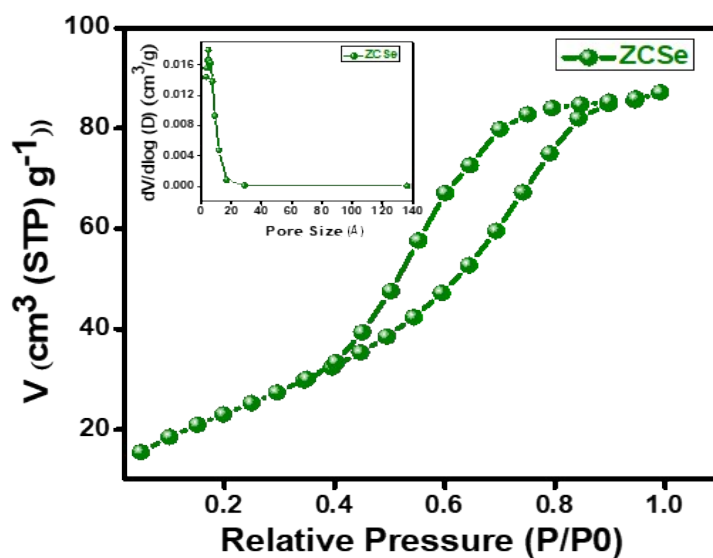


Fig. S3. BET surface area and pore size distribution of ZCSe.

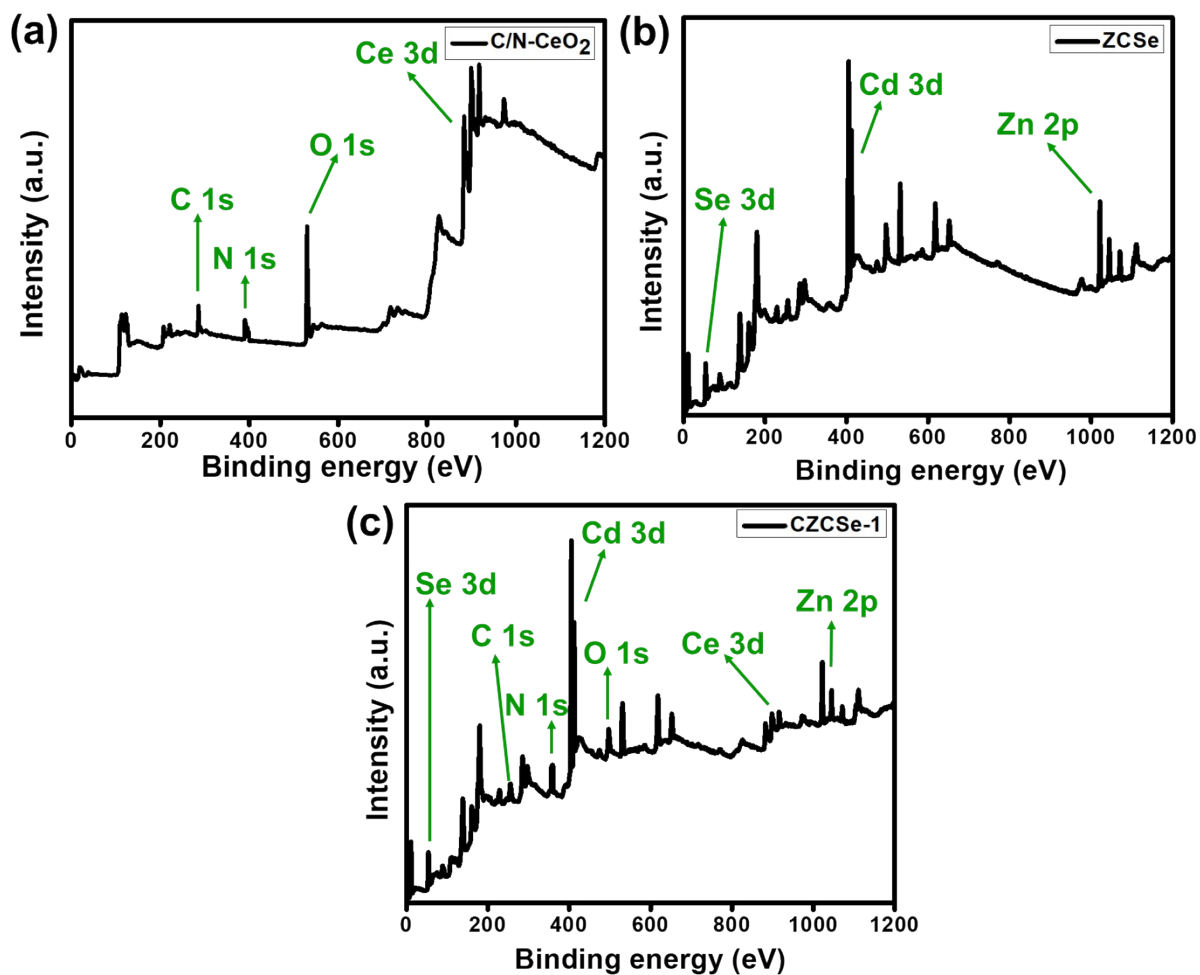


Fig. S4. XPS survey scan spectra of (a) C/N-CeO₂, (b) ZCSe, and (c) CZCSe-1

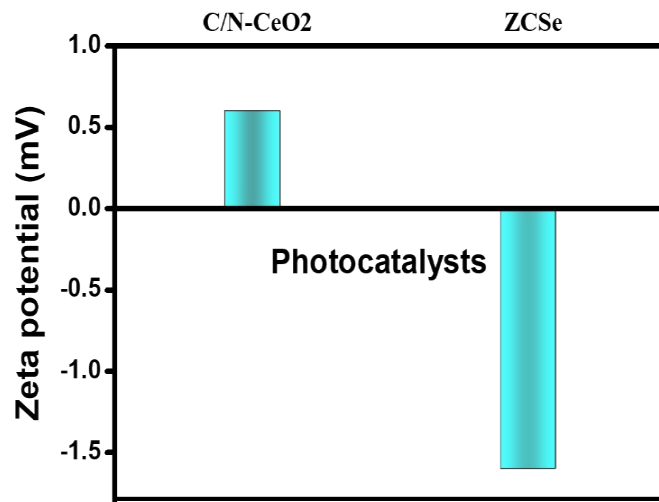


Fig. S5. Zeta potential plot of C/N-CeO₂ and ZCSe.

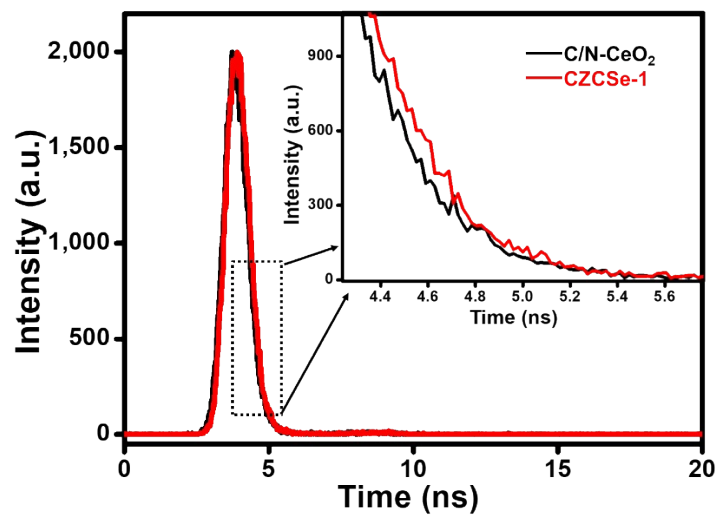


Fig. S6. TRPL plot of C/N-CeO₂ and CZCSe-1 composite

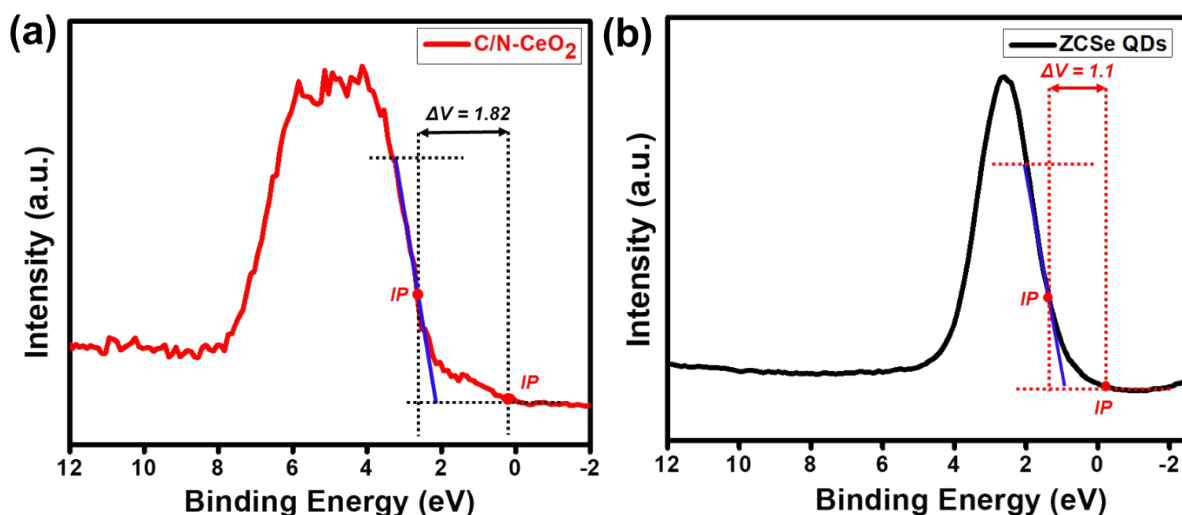


Fig. S7. Work function measured by VB-XPS (a) C/N-CeO₂ and (b) ZCSe

Table S1. XPS binding energy comparison between C/N-CeO₂, MIS, and MC-2 photocatalyst.

Binding energy (eV)									Ref.
Ce 3d									
C/N-CeO ₂	882.2	883.9	888.9	898.2	900.9	900.5	906.3	916.6	1,2
CZCSe-1	882.3	884.5	889.2	898.3	900.9	901.0	906.9	916.7	
Difference	0.1	0.6	0.3	0.1	0.0	0.5	0.6	0.1	
Reason	³ d _{3/2}	³ d _{3/2}	³ d _{3/2}	³ d _{3/2}	³ d _{5/2}	³ d _{5/2}	³ d _{5/2}	³ d _{5/2}	
O 1s									
C/N-CeO ₂	529.2				531.0				2-6
CZCSe-1	529.4				531.6				
Difference	0.2				0.6				
Reason	Lattice oxygen				Oxygen vacancy				
N 1s									
C/N-CeO ₂	399.2				401.1				5,7
CZCSe-1	399.2				401.1				
Difference	0.0				0.0				
Reason	Doped N				Interstitial N				
C 1s									
C/N-CeO ₂	284.6	285.9		289.0		4,8,9			
CZCSe-1	284.7	286.0		288.7					
Difference	0.1	0.1		0.3					
Reason	C=C	C-N		C-OH, O=C-O					
Zn 2p									
ZCSe	1044.8				1021.7				10
CZCSe-1	1044.4				1021.6				
Difference	0.4				0.1				
Reason	2p _{1/2}				2p _{3/2}				
Cd 3d									

ZCSe	411.8	405.0	10,11
CZCSe-1	411.6	404.8	
Difference	0.2	0.2	
Reason	$3d_{3/2}$	$3d_{5/2}$	
Se 3d			
ZCSe	54.5	53.7	12
CZCSe-1	54.4	53.4	
Difference	0.1	0.3	
Reason	$3d_{3/2}$	$3d_{5/2}$	

5. Scavenger test:

The trapping test was conducted to identify the active species which are responsible for the photocatalytic generation of H_2O_2 reaction. Different scavengers such as p-benzoquinone (p-BQ), tert-butyl alcohol (TBA), citric acid (CA), and dimethyl sulfoxide (DMSO) are used to verify the presence of reactive species: $\cdot O_2^-$, $\cdot OH$, h^+ , and e^- respectively. The role of different reactive species towards photocatalytic H_2O_2 production was examined and displayed in Fig. S6.

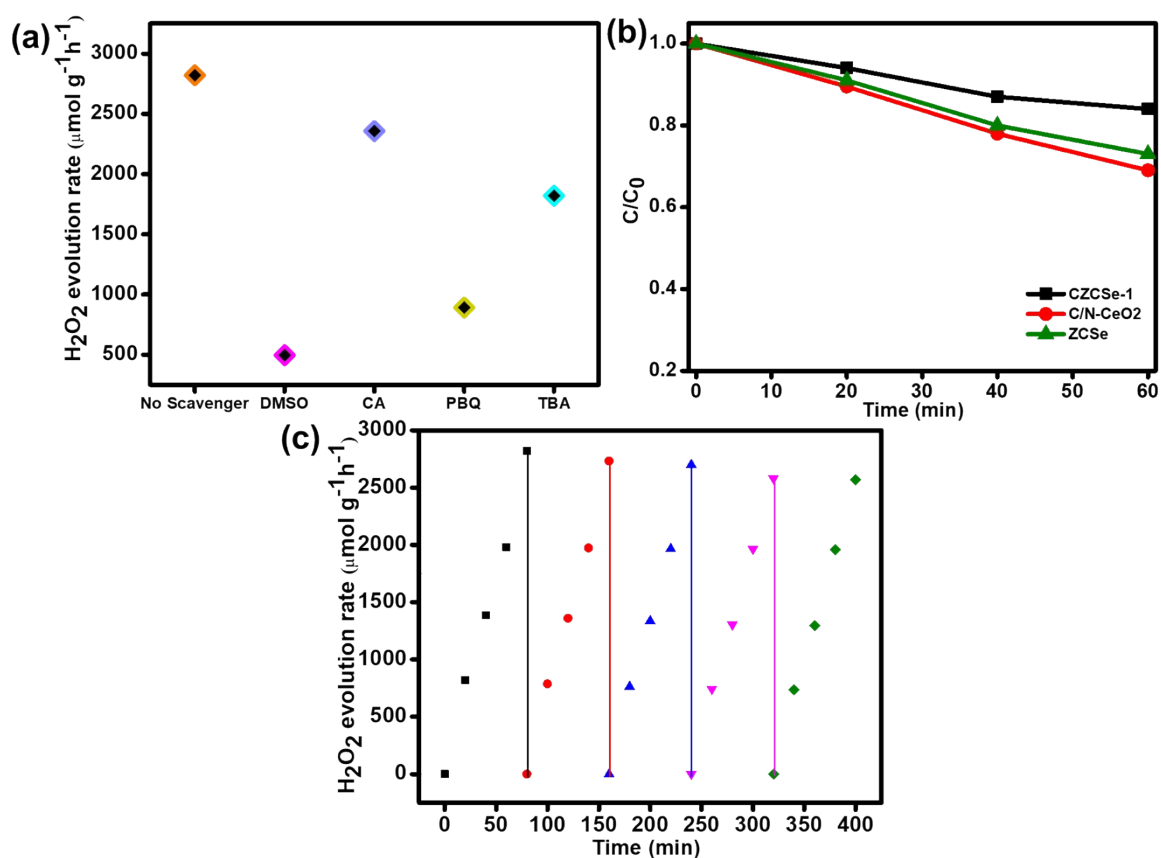


Fig. S8. (a) Photocatalytic H_2O_2 production rate in presence of different scavengers (b) decomposition of H_2O_2 over different synthesized materials (c) cycle stability test of CZCSe-1.

Over the catalyst horizon, to confirm the presence of $\cdot\text{O}_2^-$ which is the key reactive species towards H_2O_2 production and water reduction, NBT test was conducted. In this typical experiment, 10 mL of Nitro blue tetrazolium suspension ($5 \times 10^5 \text{ M}$) with 0.01 g photocatalyst was exposed to sunlight for 1 h. After the illumination period, photocatalyst was separated by centrifugation and analyzed through UV-Vis DRS as shown in Fig. S9 (a). From the spectra it can be observed that, solar light exposed NBT shows decreased absorption intensity as compare to the neat NBT which prove the presence of $\cdot\text{O}_2^-$ and hence it helps in photocatalytic production of H_2O_2 via O_2 reduction process.

Whereas, to confirm the presence of $\cdot\text{OH}$, terephthalic acid (TA) test was performed for the water oxidation reaction. In this experiment, TA reacts with OH^- to form hydroxyterephthalic acid (HTA), which confirms the presence of $\cdot\text{OH}$ in the solution. For this test, 5 mM TA was taken along with NaOH and the required amount of photocatalyst was added to the solution. The final solution was placed under sunlight for 30 min and after that, PL measurement was performed. The emission peak of composite at $\lambda = 425 \text{ nm}$ is considered as the formation of HTA complex. Above result as shown in Fig. S9 (b) concluded the presence of $\cdot\text{OH}$ in the reaction vessel which helped in O_2 evolution reaction via water splitting and moderately helps for H_2O_2 production by combining with another radical of its own.

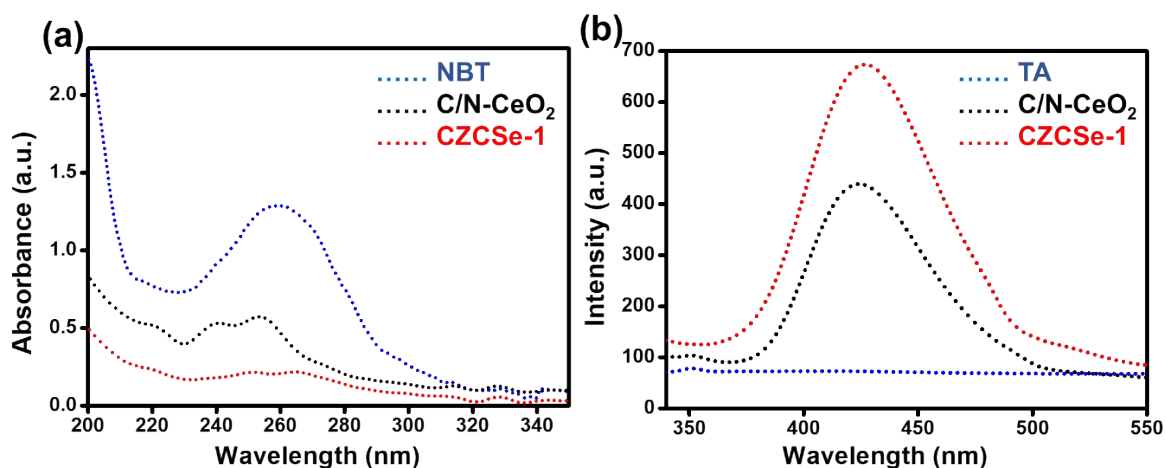


Fig. S9. (a) NBT and (b) TA Test results for neat C/N-CeO₂ and CZCSe-1

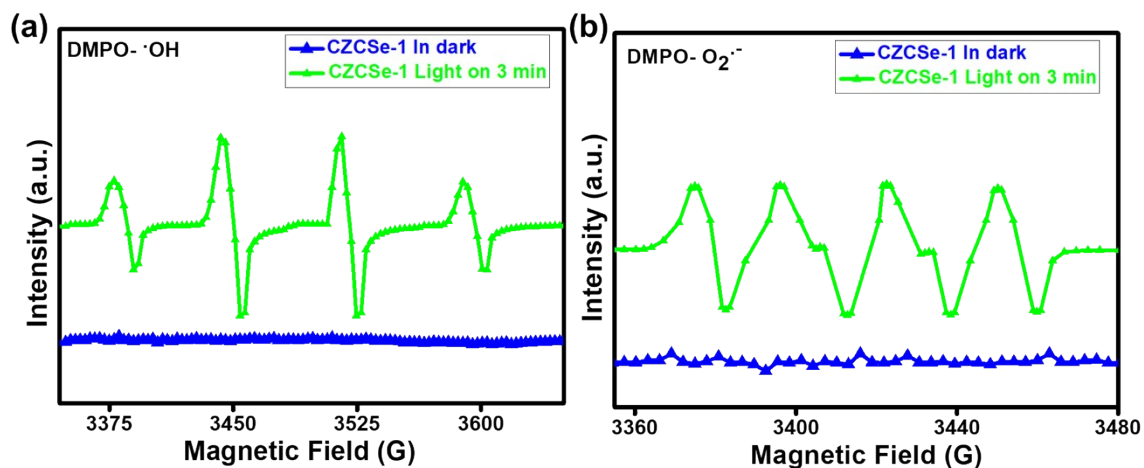


Fig. S10. EPR analysis (a) DMPO- $\cdot\text{OH}$ and (b) DMPO- $\cdot\text{O}_2^-$ for CZCSe-1 in presence and absence of light

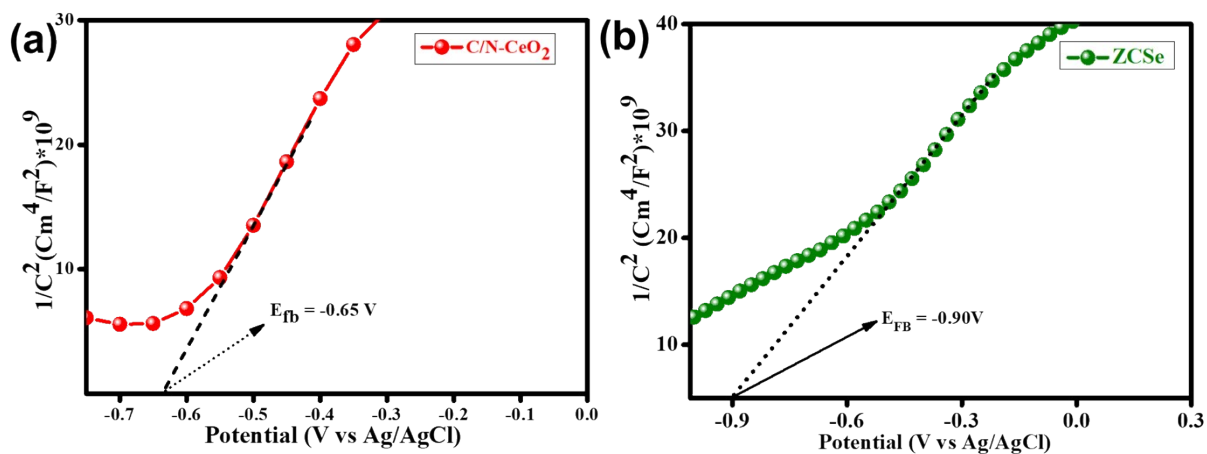


Fig. S11. Mott-schottky plot of (a) C/N-CeO₂ and (b) ZCSe for CZCSe

Table S2. BET surface area and pore volume of C/N-CeO₂, and CZCSe-1 photocatalysts.

Photocatalyst	BET surface area (m ² /g)	Pore volume (Å)			
		2.31	5.54	8.98	14.99
C/N-CeO ₂	57.045	2.31	5.54	8.98	14.99
CZCSe-1	80.2	2.26	4.58	8.70	14.91

Table S3. Respective band edge potential and optical bandgap values of C/N-CeO₂ and ZCSe.

Photocatalyst	E _{fb} vs Ag/AgCl (V)	CB vs NHE (V)	VB vs NHE (V)	Bandgap (eV)
C/N-CeO ₂	-0.65	-0.56	2.3	2.86
ZCSe	-0.9	-0.81	0.94	1.75

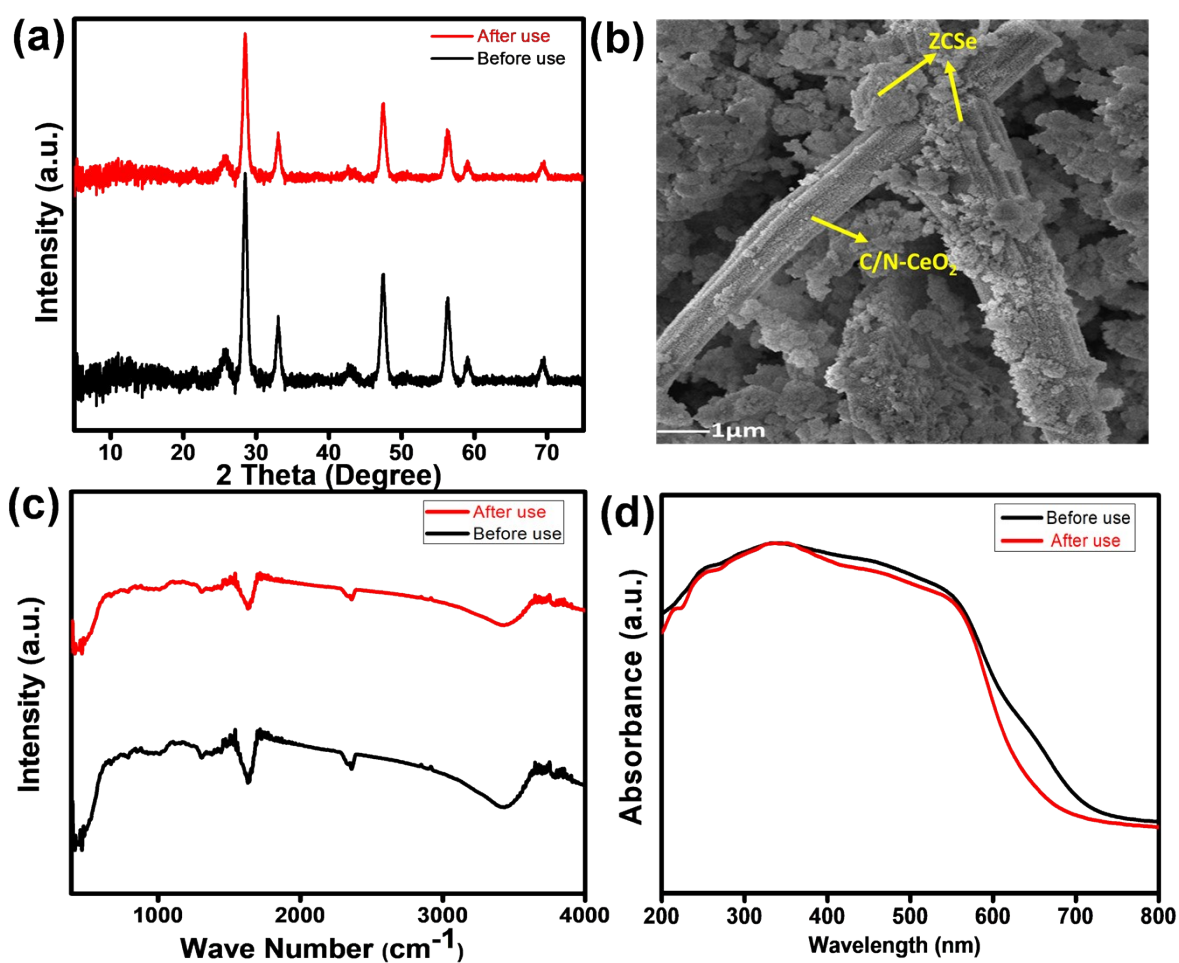
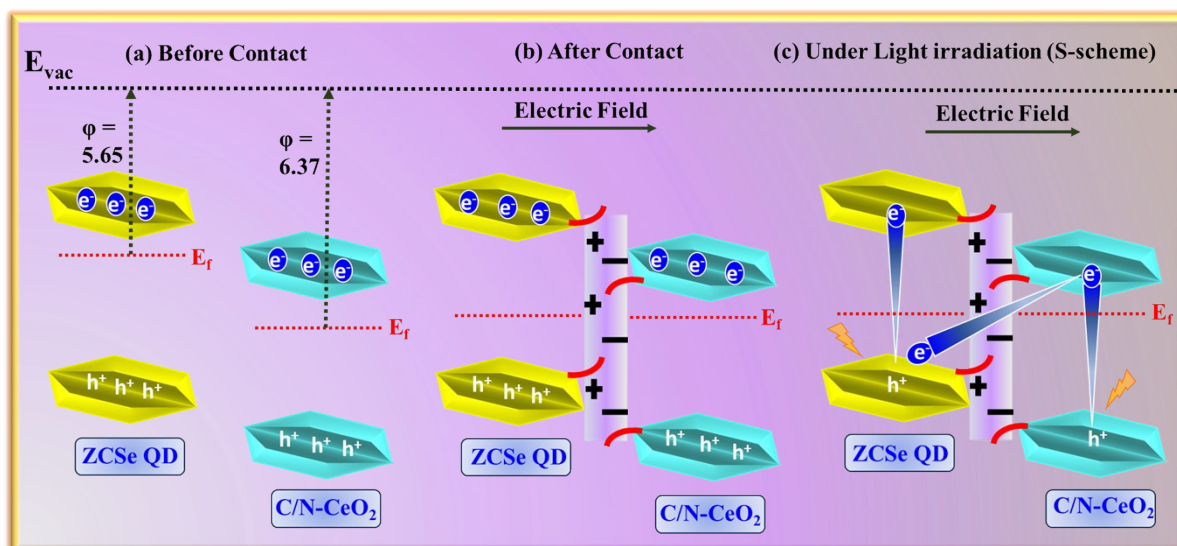


Fig. S12. Post experimental characterizations: (a) XRD, (b) FESEM, (c) FT-IR, and (d) UV-Vis spectra of CZCSe-1.



Scheme-S1 The work function of C/N-CeO₂ and ZCSe before contact. (b) The electric-field and band-edge bending at the interfacial space after interaction. (c) The S-scheme charge transmission mechanisms between C/N-CeO₂ and ZCSe under light illumination.

Table S4. Respective H₂O₂ production rate of all prepared samples using different sacrificial agent.

Photocatalysts	H ₂ O ₂ evolution rate (μmol/h/g) using different sacrificial agent		
	MeOH	EtOH	IPA
C/N-CeO ₂	1183.6	992.8	1342.5
ZCSe	1346.8	1190.5	1590
CZCSe-0.5	2283.7	2178.9	2667.12
CZCSe-1	2561.6	1254.3	2820.43
CZCSe-1.5	2315.3	2237.3	2589.46

Table S5. Comparison of photocatalytic O₂ evolution rate of different catalysts.

Photocatalyst	Light source	Sacrificial agent	O ₂ Production rate (μmol/h)	Ref.
CuO/CeO ₂	300 W Xe lamp	NaOH and Na ₂ S ₂ O ₈	19.6	13
α-MnO ₂ @B/O-g-	150 W Hg lamp	AgNO ₃	295.1	14

C ₃ N ₄				
ZnCr ₂ O ₄ @ZnO/g-C ₃ N ₄	Visible light ($\lambda \geq 400$ nm)	AgNO ₃	227.5	15
CeO ₂ /UNH (Ce)	125 W Hg lamp	FeCl ₃	370.2	1
C/N- CeO ₂ /MIS	125 W Hg lamp	AgNO ₃	210.1	9
C/N- CeO ₂ /ZCSe	125 W Hg lamp	AgNO ₃	234.89	This work

Table S6. Comparison of photocatalytic H₂O₂ production rate of different catalysts.

Photocatalyst	Light source	Sacrificial agent	H ₂ O ₂ Production rate ($\mu\text{mol/g/h}$)	Ref.
CeO ₂ / SnIn ₄ S ₈	Visible light	No sacrificial agent	33.6	16
C/N-ZnO@NixPy	250 W Hg lamp	Ethanol	2495.1 \pm 62.3	17
MgIn ₂ S ₄ @BCN	250 W Hg lamp	Ethanol	2175	18
TiO ₂ @MXene/B-g-C ₃ N ₄	250 W Hg lamp	Ethanol	1480.1	19
Fe ₂ O ₃ /BCN	250 W Hg lamp	IPA	729	20
Mn ₃ O ₄ /Co ₉ S ₈	Xe lamp > 420 nm	Ethanol	1020	21
C/N- CeO ₂ /MIS	250 W Hg lamp	IPA	2520.4	9
C/N- CeO ₂ /ZCSe	250 W Hg lamp	IPA	2820.43	This work

Table S7. Details of Chemicals and Instruments used.

Sl No.	Chemicals/ Instruments	Manufacturer	City and Country
1	Cerium chloride, 2-Amino-1,4-benzenedicarboxylic acid, Magnesium nitrate, Indium nitrate, Thioacetamide	Sigma-Aldrich	Burlington, United states
2	Methanol, and N, N- Dimethyl	Merck	Darmstadt, Germany

	formamide		
3	X-Ray Diffraction (XRD)	Rigaku-Ultima IV	Tokyo, Japan
4	UV–Visible (UV–Vis) diffuse reflectance spectra (DRS)	JASCO V-750	Halifax, Canada
5	Fourier Transform Infrared spectrometer (FTIR)	JASCO FTIR-4600	Halifax, Canada
6	Photoluminescence Spectrofluorometer (PL)	JASCO FP-8300 spectrofluorometer	Halifax, Canada
7	Raman spectrometer	RENISHAW InVia Raman spectrometer	Wotton-under-Edge, England
8	Electrochemical analyser	IVIUMnSTAT	Eindhoven, Netherland
9	Transmission electron microscopy (TEM)	TEM,JEOL-2100	Tokyo, Japan
10	Field Emission Scanning Electron Microscope (FESEM)	Zeiss, Gemini-300	Jena, Germany
11	Electron paramagnetic resonance spectrometer (EPR)	Bruker, ELEXSYS	Billerica, United states
12	Zeta potential	Zetasizer Nano ZS	Malvern, United Kingdom

References

- 1 S. Mansingh, S. Subudhi, S. Sultana, G. Swain and K. Parida, *ACS Appl Nano Mater*, 2021, **4**, 9635–9652.
- 2 S. Sultana, S. Mansingh and K. M. Parida, *Journal of Physical Chemistry C*, 2018, **122**, 808–819.
- 3 S. P. Tripathy, S. Subudhi, A. Ray, P. Behera, A. Bhaumik and K. Parida, *Langmuir*, 2022, **38**, 1766–1780.
- 4 S. Mansingh, S. Subudhi, S. Sultana, G. Swain and K. Parida, *ACS Appl Nano Mater*, 2021, **4**, 9635–9652.
- 5 S. Subudhi, G. Swain, S. P. Tripathy and K. Parida, *Inorg. Chem.* 2020, **59**, 9824–9837.
- 6 B. P. Mishra, L. Acharya, S. Subudhi and K. Parida, *Int J Hydrogen Energy*, 2022, **47**, 32107–32120.
- 7 X. Cheng, X. Yu and Z. Xing, *Appl Surf Sci*, 2012, **258**, 3244–3248.
- 8 A. Ray, S. Subudhi, S. P. Tripathy, L. Acharya and K. Parida, *Adv Mater Interfaces*, 2022, **34**, 2201440.
- 9 J. Panda, P. Behera, S. Subudhi, S. P. Tripathy, G. Swain, S. Dash and K. Parida, *Mater Adv*, 2024, **5**, 4865–4877.
- 10 N. X. Ca, H. T. Van, P. V. Do, L. D. Thanh, P. M. Tan, N. X. Truong, V. T. K. Oanh, N. T. Binh and N. T. Hien, *RSC Adv*, 2020, **10**, 25618–25628.
- 11 M. Yang, Y. Wang, Y. Ren, E. Liu, J. Fan and X. Hu, *J Alloys Compd*, 2018, **752**, 260–266.
- 12 V. I. Markoulaki, I. T. Papadas, I. Kornarakis and G. S. Armatas, *Nanomaterials*, 2015, **5**, 1971–1984.
- 13 V. I. Markoulaki, I. T. Papadas, I. Kornarakis and G. S. Armatas, *Nanomaterials*, 2015, **5**, 1971–1984.
- 14 B. P. Mishra, L. Acharya, S. Subudhi and K. Parida, *Int J Hydrogen Energy*, 2022, **47**, 32107–32120.
- 15 S. Patnaik, D. P. Sahoo, L. Mohapatra, S. Martha and K. Parida, *Energy Technology*, 2017, **5**, 1687–1701.
- 16 Y. Xiao, Y. Tao, Y. Jiang, J. Wang, W. Zhang, Y. Liu, J. Zhang, X. Wu and Z. Liu, *Sep Purif Technol*, 2022, **623**, 109-123.

- 17 A. Ray, S. Subudhi, S. P. Tripathy, L. Acharya and K. Parida, *Adv Mater Interfaces*, 2022, **34**, 2201440.
- 18 L. Acharya, G. Swain, B. P. Mishra, R. Acharya and K. Parida, *ACS Appl Energy Mater*, 2022, **5**, 2838–2852.
- 19 B. P. Mishra, L. Biswal, S. Das, L. Acharya and K. Parida, *Langmuir*, 2023, **39**, 957–971.
- 20 Z. Lu, X. Zhao, Z. Zhu, Y. Yan, W. Shi, H. Dong, Z. Ma, N. Gao, Y. Wang and H. Huang, *Chemistry - A European Journal*, 2015, **21**, 18528–18533.
- 21 H. Zhang and X. Bai, *Appl Catal B*, 2021, **298**, 120516.